

Special Issue Article

Bacteria associated with wood tissues of Esca-diseased grapevines: functional diversity and synergy with *Fomitiporia mediterranea* to degrade wood components

Rana Haidar ^{1,2*}, Amira Yacoub,¹ Jessica Vallance,¹ Stéphane Compant,³ Livio Antonielli,³ Ahmad Saad,⁴ Birgit Habenstein,⁴ Brice Kauffmann,⁵ Axelle Grélar,⁴ Antoine Loquet,⁴ Eléonore Attard,⁶ Rémy Guyoneaud⁶ and Patrice Rey¹

¹INRAE, UMR SAVE, Bordeaux Science Agro, ISVV, University of Bordeaux, Villenave d'Ornon, 33882, France.

²Biology Department, Faculty of Science, Tishreen University, Latakia, Syria.

³AIT Austrian Institute of Technology GmbH, Bioresources Unit, Center for Health and Bioresources, Konrad Lorenz Straße 24, Tulln, 3430, Austria.

⁴Institut de Chimie et Biologie des Membranes et des Nanoobjets, IECB, CNRS, Université de Bordeaux, Pessac, 33607, France.

⁵IECB, UMS 3033, US001, CNRS, Université de Bordeaux, Pessac, 33607, France.

⁶Université de Pau et des Pays de l'Adour/E2S UPPA/ CNRS, Institut des Sciences Analytiques et de Physicochimie pour l'Environnement et les Matériaux – UMR 5254, IBEAS Avenue de l'Université, Pau, 64013, France.

Summary

Fungi are considered to cause grapevine trunk diseases such as esca that result in wood degradation. For instance, the basidiomycete *Fomitiporia mediterranea* (*Fmed*) is overabundant in white rot, a key type of wood-necrosis associated with esca. However, many bacteria colonize the grapevine wood too, including the white rot. In this study, we hypothesized that bacteria colonizing grapevine wood interact, possibly synergistically, with *Fmed* and enhance

the fungal ability to degrade wood. We isolated 237 bacterial strains from esca-affected grapevine wood. Most of them belonged to the families *Xanthomonadaceae* and *Pseudomonadaceae*. Some bacterial strains that degrade grapevine-wood components such as cellulose and hemicellulose did not inhibit *Fmed* growth *in vitro*. We proved that the fungal ability to degrade wood can be strongly influenced by bacteria inhabiting the wood. This was shown with a cellulolytic and xylanolytic strain of the *Paenibacillus* genus, which displays synergistic interaction with *Fmed* by enhancing the degradation of wood structures. Genome analysis of this *Paenibacillus* strain revealed several gene clusters such as those involved in the expression of carbohydrate-active enzymes, xylose utilization and vitamin metabolism. In addition, certain other genetic characteristics of the strain allow it to thrive as an endophyte in grapevine and influence the wood degradation by *Fmed*. This suggests that there might exist a synergistic interaction between the fungus *Fmed* and the bacterial strain mentioned above, enhancing grapevine wood degradation. Further step would be to point out its occurrence in mature grapevines to promote esca disease development.

Introduction

Esca, a grapevine trunk disease (GTD), has become a major issue in many viticulture regions in Europe, and even worldwide, in the past two decades. This disease negatively affects vineyard longevity and wine quality (Mugnai *et al.*, 1999; Calzarano *et al.*, 2001, 2004; Pasquier *et al.*, 2013), thereby causing huge economic losses to the viticulture sector. Pathogenic fungi such as *Phaeoconiella chlamydospora*, *Phaeoacremonium minimum* and *Fomitiporia mediterranea* (*Fmed*) have long been studied for their ability to colonize and degrade wood tissues, causing various types of symptoms in the wood of trunk and stems (Mugnai *et al.*, 1999; Sparapano

Received 20 November, 2020; accepted 18 July, 2021. *For correspondence. E-mail haidarrana@gmail.com; Tel. (+33) 05 57 12 26 24.

et al., 2001; Fischer, 2002; Laveau et al., 2009). These symptoms include central or sectorial black and/or brown necrotic tissues and also white-rot tissues (Larignon and Dubos, 1997; Mugnai et al., 1999; Serra et al., 2000; Péros et al., 2008; Maher et al., 2012). White rot in grapevine is always associated with basidiomycetes. A considerable number of basidiomycetes have been isolated from different grapevine cultivars worldwide (Mugnai et al., 1999; Fischer, 2006; Cloete et al., 2014; Brown et al., 2020; Mirabolfathy et al., 2021), which are known to degrade the components of cell walls, i.e. lignin, cellulose and hemicellulose.

Fomitiporia mediterranea (Fischer, 2002) is the most common basidiomycete associated with white-rot tissues, typically esca, in grapevine plants in Europe. It is assumed that the development of wood decay, including white-rot, is a long process that takes place over years (Sparapano et al., 2000, 2001). As vineyards age, white rot continues to spread in the trunks and cordons of grapevine plants (Fischer, 2000; Fischer and González Garcia, 2015). Recent findings support the idea that white-rot plays a key role in causing esca. In esca-affected plants displaying leaf symptoms, at least 10% of wood had been affected by white rot (Ouadi et al., 2021), and removal of the white-rot led to grapevine recovery (Cholet et al., 2021).

It was reported that in asymptomatic young grapevines (10-years-old), the healthy-looking wood was colonized by the three fungal pathogens, *P. chlamydospora*, *P. minimum* and *F. mediterranea* (Bruez et al., 2014, 2020; Kraus et al., 2019). In addition, numerous non-pathogenic fungi were also detected, including some plant-protective microorganisms such as *Trichoderma* spp. (Fourie et al., 2001; Bruez et al., 2014; Mutawila et al., 2016; Marraschi et al., 2018). Healthy wood tissues exhibited a higher fungal diversity in comparison to the necrotic ones. However, which factors cause necrosis of the healthy and young grapevine woods (10-years-old) after few years (in 15–20-years-old grapevines) are yet unknown.

In this study, we hypothesized that one of these factors influencing wood degradation, in addition to pathogenic fungi, could be the synergistic interaction of these fungi with certain bacteria that colonize the wood of grapevines (Bruez et al., 2015, 2020). This assumption was raised because some authors, such as Clausen (1996) reported that bacteria can affect negatively wood permeability, change wood structure, or work synergistically with other wood-inhabiting bacteria and soft-rot fungi to predispose wood to fungal attack. Therefore, the possible involvement of grapevine wood-colonizing bacteria, alone or in association with GTD-fungal pathogens, could be possible and needs therefore to be further investigated to determine if they are involved in grapevine wood

degradation. A multipartite interaction, or a pathobiome, consisting of fungi and bacteria, could be studied further to determine if it can increase the rate of pathogenic fungi-induced wood degradation.

Fungi are generally considered as primary decomposers of wood because of their ability to produce a wide range of extracellular enzymes that degrade major wood polymers, i.e. lignin, cellulose and hemicellulose (Clausen, 1996; Boer et al., 2005; Noll and Jirjis, 2012; Purahong et al., 2016). Due to the limited ability of bacteria to decompose polymeric lignocelluloses, they were thought to play only a minor role in wood decomposition compared to fungi (Cornelissen et al., 2012). However, genomic analyses of certain bacteria revealed the existence of genes encoding lignin-degrading enzymes, suggesting their possible involvement in wood decomposition (Lladó et al., 2017).

Recent studies have reported that some of the wood-colonizing bacteria play a positive role of plant protection by reducing the size of the wood necroses caused by GTD-pathogens (Rezgui et al., 2016; Haidar et al., 2016a; Haidar et al., 2016b). However, some of these bacteria, such as strains of *Bacillus pumilus*, *Xanthomonas* sp. and *Bacillus licheniformis*, might develop synergistic relationships with *Neofusicoccum parvum*, which is considered as one of the most virulent fungal species associated with GTDs (Laveau et al., 2009; Úrbez-Torres and Gubler, 2009). Recently, it was reported that bacterial inoculation favours the pathogenicity of *N. parvum* by increasing canker length in grapevine stem cuttings (Haidar et al., 2020). However, as regards esca, no study has yet been conducted on the interaction between bacteria and *Fmed*. The present study was aimed at (i) determining if bacteria isolated from grapevine wood can degrade the wood structure of this plant even minimally, then (ii) we tested the hypothesis that an interaction, possibly synergistic, between wood-colonizing bacteria and *Fmed*, might eventually lead to increased wood structure degradation.

Results

Characterization of the bacterial strains isolated from the grapevine wood tissues

Identification by 16S rRNA gene sequencing. A total of 237 bacterial strains were isolated from different tissues of grapevine: 59 strains from necrotic (sectorial black streaks) tissues (NT), 62 strains from non-necrotic tissues (NNT), 54 strains from transition tissues between necrotic and non-necrotic zones (TT) and 62 strains from white rot (decaying wood) tissues (WR).

All strains were identified by sequencing a fragment of the 16S rRNA gene (V5–V9 region). Sequences are

available at the GenBank database from accession number MT705336 to MT705572.

The sequences revealed that the 237 isolates belonged to four phyla: *Proteobacteria* (64% of the isolates), *Firmicutes* (21%), *Bacteroidetes* (10%) and *Actinobacteria* (5%). Furthermore, among the 11 obtained bacterial orders the ones with the highest number of strains were *Xanthomonadales*, *Bacillales* and *Pseudomonadales* with 30.8%, 21.1% and 18.6% of the bacterial strains respectively. Thirty-one genera were also identified. The most frequently occurring genera were *Pseudomonas* (18.6% of the bacterial strains), followed by *Stenotrophomonas* (13%), *Bacillus* (12.6%) and *Pseudoxanthomonas* (12.6%).

While some strains belonging to genera such as *Bacillus*, *Olivibacter*, *Pseudomonas* and *Pseudoxanthomonas* were present in all wood tissues, strains of other genera such as *Herbiconiux* and *Kocuria* were isolated from only one type of tissue, i.e. white rot tissue, and those of *Burkholderia*, *Curtobacterium*, *Luteibacter*, *Pantoea*, *Rahnella* and *Rhizobium* were isolated only from non-necrotic tissue. Figure 1 shows the distribution of the most abundant genera and according to the wood tissues sampled from trunk or cordon.

Ability of the selected bacterial strains to decompose wood components. A total of 59 taxa were defined when sequences were binned into taxa (Gascuel, 1997;

Edgar, 2004). One bacterial strain from each taxon was selected for further analyses (Table 1).

None of these strains was able to degrade the Remazol Brilliant Blue R (RBBR) dye, suggesting the absence of ligninolytic activity. Cellulase and xylanase activities were evaluated according to the extent and intensity of hydrolytic clearing zones, classified as moderate (5–40 mm), strong (41–70 mm) and very strong (>71 mm). The screening confirmed 18 strains (30%) showing cellulase and xylanase activity halos with a diameter >5 mm in a Congo Red assay on xylan- and carboxymethyl-cellulose-containing plates (Fig. S1). Ten of these strains were isolated from trunks and eight from cordons. While seven of these 18 strains were isolated from white rot (S136, S158, S159, S190, S23, S283 and S68), only two were isolated from non-necrotic tissues (S241: *B. muralis* and S293: *Paenibacillus amylolyticus*) (Table 1). Strain S150 was the only strain (isolated from the transition tissue of one cordon) that showed strong cellulase and xylanase activities.

Only 11 strains (S107, S11, S195, S196, S2, S207, S22, S233, S300, S47 and S5), i.e. 18% of the screened strains, demonstrated cellulolytic activity. Six of these were isolated from non-necrotic tissues. However, eight other strains (S126, S211, S222, S243, S252, S259, S69 and S92) showed only xylanolytic potential by forming zones of clearing on xylan containing plates; none of these strains was isolated from white rot (Table 1).

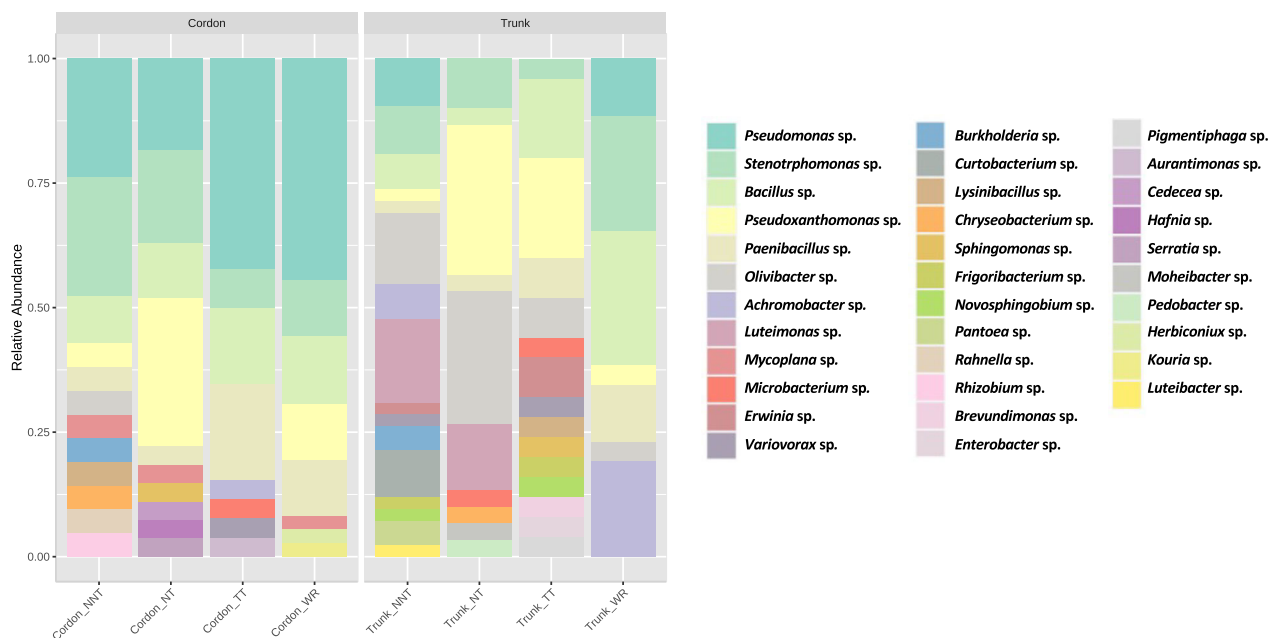


Fig. 1. Distribution of bacterial genera in the different wood tissue types. Necrotic tissues (sectorial black streaks) (NT), non-necrotic tissues (NNT), transition tissues between the necrotic and non-necrotic zones (TT) and white rot (decay wood) (WR), a typical necrotic tissue associated with esca. [Color figure can be viewed at wileyonlinelibrary.com]

Table 1. *In vitro* wood components degradation and *Fmed* mycelial growth inhibition by 59 bacterial strains isolated from wood tissues of grapevines.

Test code	Bacterial species	Bacterial origin	Degradation (halo size mm)			Inhibition rate (%)	
			Lignin	Cellulose	Xylan	Dual culture trial	VOCs emission trial
S163	<i>Microbacterium</i> sp.	Necrotic tissue of trunk	0	0	0	0	100
S45	<i>Pseudomonas</i> sp.	Non-necrotic tissue of trunk	0	0	0	52.5	75.9
S7	<i>Sphingomonas</i> sp.	Intermediate zone of trunk	0	0	0	2.5	46.2
S180	<i>Stenotrophomonas</i> sp.	Non-necrotic tissue of cordon	0	0	0	52.3	88.8
S273	<i>Bacillus</i> sp.	Intermediate zone of trunk	0	0	0	0	66.6
S12	<i>Stenotrophomonas</i> sp.	Non-necrotic tissue of cordon	0	0	0	28.8	74
S256	<i>Luteimonas</i> sp.	Necrotic tissue of trunk	0	0	0	0	81.4
S262	<i>Achromobacter</i> sp.	Non-necrotic tissue of trunk	0	0	0	41	85.1
S125	<i>Brevundimonas</i> sp.	Intermediate zone of trunk	0	0	0	0	66.6
S112	<i>Novosphingobium</i> sp.	Non-necrotic tissue of trunk	0	0	0	55.1	100
S64	<i>Herbiconiux</i> sp.	White rot of cordon	0	0	0	0	66.6
S62	<i>Kocuria</i> sp.	White rot of cordon	0	0	0	0	74
S46	<i>Curtobacterium</i> sp.	Non-necrotic tissue of trunk	0	0	0	45.2	100
S261	<i>Erwinia</i> sp.	Non-necrotic tissue of trunk	0	0	0	15	88
S174	<i>Frigoribacterium</i> sp.	Intermediate zone of trunk	0	0	0	49.7	66
S172	<i>Lysinibacillus</i> sp.	Intermediate zone of trunk	0	0	0	36.3	61.1
S146	<i>Rahnella</i> sp.	Non-necrotic tissue of cordon	0	0	0	22.5	100
S123	<i>Erwinia</i> sp.	Intermediate zone of trunk	0	0	0	23.4	100
S178	<i>Burkholderia</i> sp.	Non-necrotic tissue of cordon	0	0	0	0	88.8
S298	<i>Pseudomonas</i> sp.	Intermediate zone of cordon	0	0	0	17.5	66.6
S165	<i>Burkholderia</i> sp.	Non-necrotic tissue of trunk	0	0	0	0	55.5
S151	<i>Mycoplana</i> sp.	White rot of cordon	0	0	0	26	77.7
S259	<i>Weeksellaceae</i>	Necrotic tissue of trunk	0	0	90	-5.1	62.9
S243	<i>Hafnia</i> sp.	Non-necrotic tissue of cordon	0	0	90	16.8	83.3
S252	<i>Stenotrophomonas</i> sp.	Intermediate zone of cordon	0	0	90	23.7	87
S222	<i>Pantoea</i> sp.	Non-necrotic tissue of trunk	0	0	70	44.4	75
S92	<i>Pseudomonaceae</i>	Intermediate zone of cordon	0	0	60	44.1	100
S211	<i>Pseudoxanthomonas</i> sp.	Necrotic tissue of trunk	0	0	90	2.2	0
S69	<i>Pseudoxanthomonas</i> sp.	Necrotic tissue of trunk	0	0	50	12	100
S126	<i>Bacillus</i> sp.	Intermediate zone of trunk	0	0	70	0	72.2
S22	<i>Achromobacter</i> sp.	White rot of cordon	0	15	0	36	83.3
S203	<i>Olivibacter</i> sp.	Necrotic tissue of trunk	0	20	90	0	62.9
S270	<i>Paenibacillus</i> sp.	Intermediate zone of trunk	0	20	70	-4.7	64.8
S300	<i>Rhizobiaceae</i>	Non-necrotic tissue of cordon	0	20	0	4.6	57.4
S274	<i>Pigmentifaga</i> sp.	Intermediate zone of trunk	0	20	30	0	55.5
S107	<i>Pedobacter</i> sp.	Necrotic tissue of trunk	0	20	0	0	55.5
S2	<i>Variovorax</i> sp.	Non-necrotic tissue of trunk	0	25	0	32.5	55.5
S127	<i>Luteimonas</i> sp.	Intermediate zone of trunk	0	30	70	16.2	88.8
S195	<i>Achromobacter</i> sp.	White rot of trunk	0	30	0	23	51.8
S207	<i>Pseudomonas</i> sp.	Non-necrotic tissue of trunk	0	30	0	0	64.8
S142	<i>Cedecea</i> sp.	Necrotic tissue of cordon	0	30	60	2.3	75.9
S233	<i>Pseudoxanthomonas</i> sp.	Necrotic tissue of cordon	0	35	0	19.8	83.3
S11	<i>Enterobacter</i> sp.	Non-necrotic tissue of cordon	0	35	0	-15.8	44.4
S47	<i>Olivibacter</i> sp.	Non-necrotic tissue of trunk	0	40	0	12.8	55.5
S190	<i>Bacillus</i> sp.	White rot of trunk	0	40	90	4.6	88.8
S5	<i>Bacillus</i> sp.	Non-necrotic tissue of trunk	0	45	0	-13.4	88.8
S231	<i>Chryseobacterium</i> sp.	Necrotic tissue of cordon	0	50	90	0	9.2
S136	<i>Pseudomonas</i> sp.	White rot of cordon	0	50	70	0	66.6
S293	<i>Paenibacillus</i> sp.	Non-necrotic tissue of cordon	0	50	75	0	11.1
S196	<i>Achromobacter</i> sp.	White rot of trunk	0	50	0	62.8	100
S23	<i>Xanthomonaceae</i>	White rot of cordon	0	50	60	30.1	83.3

(Continues)

Table 1. Continued

Test code	Bacterial species	Bacterial origin	Degradation (halo size mm)			Inhibition rate (%)	
			Lignin	Cellulose	Xylan	Dual culture trial	VOCs emission trial
S150	<i>Paenibacillus</i> sp.	Intermediate zone of cordon	0	50	90	–16.6	11.1
S241	<i>Bacillus</i> sp.	Non-necrotic tissue of cordon	0	50	60	0	61.1
S124	<i>Paenibacillus</i> sp.	Intermediate zone of trunk	0	50	90	7.1	72.2
S283	<i>Xanthomonaceae</i>	White rot of cordon	0	60	75	36.3	100
S159	<i>Bacillus</i> sp.	White rot of cordon	0	60	60	55.7	48.1
S68	<i>Paenibacillus</i> sp.	White rot of cordon	0	60	80	0	55.5
S158	<i>Bacillus</i> sp.	White rot of cordon	0	60	60	55.7	48.1
S75	<i>Bacillus</i> sp.	Necrotic tissue of cordon	0	70	90	0	77.7

In addition, we tested wood-degrading components ability of the used strain of *F. mediterranea*. This last showed ligninolytic, cellulolytic and xylanase activities.

In vitro antifungal assays

The effects of the selected bacterial strains against *Fmed* were evaluated using dual culture tests. Fifty-nine per cent of these bacterial strains (35 of 59 strains) were effective in suppressing *Fmed* (Table 1). Out of the 35 strains, only six (S112, S158, S159, S180, S196 and S45), all of which were isolated from non-necrotic tissues or white rot, showed more than 50% inhibition of radial fungal growth. Interestingly, five strains (S11, S150, S259, S270 and S5) were able to promote the mycelial growth of *Fmed*. Most of the bacterial strains (99%) exhibited antifungal activity against *Fmed* by the secretion of volatile compounds (VOCs) (Table 1).

After 7 days of incubation, there was a 100% inhibition of mycelial growth in *Fmed* due to VOCs produced by nine strains (S112, S123, S146, S163, S196, S283, S46, S69 and S92). Interestingly, eight of these strains (except

S163, i.e. *Microbacterium* sp.) reduced the mycelial growth of *Fmed*, by additionally producing diffusible antifungal substances. There was a percentage reduction in mycelial growth ranging from 12% to 62.8%. In addition, 13 other bacterial strains (S127, S178, S180, S190, S22, S23, S233, S243, S252, S256, S261, S262 and S5) showed an inhibition rate of >80%. In conclusion, 34 bacterial strains, which were isolated from different wood tissues (NNT: 13, TT: 9, NT: 3 and WR: 9), exhibited antifungal activity against *Fmed* by producing diffusible and volatile metabolites. However, S150, the strain that exhibited strong cellulase and xylanase activities and promoted mycelial growth of *Fmed*, was selected for exploring the potential synergistic interaction between the two (Table 1).

Lignin content of grapevine wood exposed to *Fmed*

While the average content of Klason lignin was 16.3% in control blocks (throughout the experiment), in blocks exposed to *Fmed* for 2, 7 and 10 months they were about 15.2%, 11.6% and 7.6% respectively (Fig. 2). Thus, the

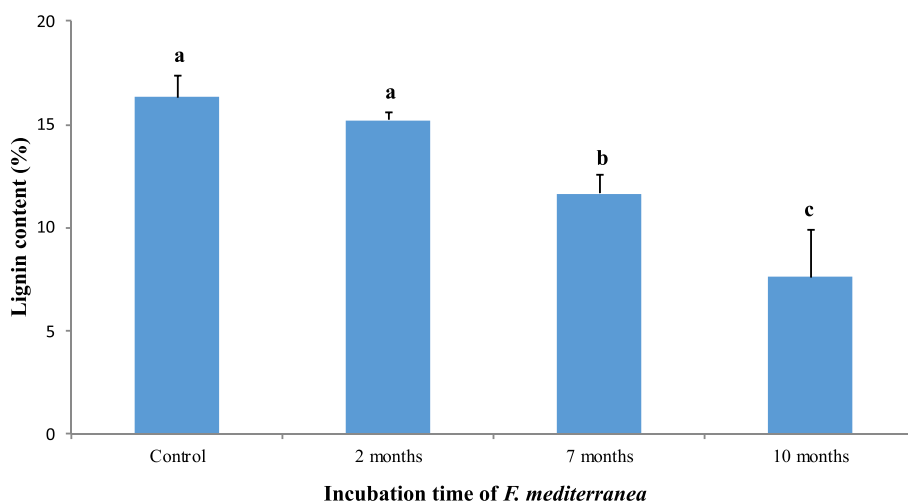


Fig. 2. Lignin content in grapevine wood exposed or not (Control) to *Fmed* after different times of incubation in laboratory. [Color figure can be viewed at wileyonlinelibrary.com]

content of Klason lignin in woodblocks exposed to *Fmed* decreased significantly with time. While incubation for 2 months showed a non-significant decrease in lignin content, incubation for 7 and 10 months significantly decreased the lignin content. In addition, we observed that the growth of *Fmed* (diameter of the colony) was improved in the presence of woodblocks, compared to that in control plates containing a culture of *Fmed* alone (Fig. S2).

Effect of Fmed and/or Paenibacillus sp. (strain S150) on grapevine wood powder in Erlenmeyer flask microcosms

To test the hypothesis that some bacteria synergistically interact with *Fmed* and that this interaction could be involved in wood degradation, sawdust co-inoculated with *Fmed* and S150 was analyzed after 2 months of incubation. The choice of this bacterial strain (S150) was based on its cellulolytic and xylanolytic activities and the fact that its metabolites cannot inhibit the growth of *Fmed*. Moreover, incubation of the fungus with S150 showed an increase in fungal growth. As qualitative indicators of wood degradation (Hervé *et al.*, 2014, 2016), we compared the color and particle size of sawdust with and without *Fmed* inoculation. We observed that sawdust inoculated with *Fmed* alone or with *Fmed* and the bacterial strain showed particles that were smaller in size and lighter in color than control sawdust, 2 months after inoculation (Fig. S3). In addition, carbon and nitrogen concentrations were measured at the end of the experimentation period (2 months after inoculation). The carbon-to-nitrogen (C/N) ratio was significantly higher in sterile sawdust (control) and in sawdust inoculated with S150 only, compared with that in sawdust inoculated with *Fmed* alone or co-inoculated with S150 (Fig. S3). In addition, the degradation of co-inoculated sawdust was significantly higher compared to sawdust inoculated with *Fmed* alone, confirming the synergy between the bacterial strain and *Fmed* and the resulting increase in wood degradation.

Effect of Fmed and/or S150 on grapevine wood powder in Petri plate microcosms

After 8 months of incubation, sawdust from Petri plate microcosms with and without *Fmed* inoculation was analyzed. The C/N ratio was found to be significantly higher in sterile sawdust (control) compared to other treatments (*Fmed*, S150 and *Fmed* with S150) indicating that the chemical composition of wood was altered by the presence of microorganisms during the period of incubation (Fig. 3A). Additionally, when compared to sawdust inoculated with *Fmed* alone, the degradation of sawdust co-inoculated with *Fmed* and S150 was significantly higher

(Fig. 3A). Furthermore, sawdust co-inoculated with *Fmed* and S150 was lighter in color compared to those inoculated with *Fmed* only (Fig. 3B). These results confirmed a synergistic interaction between S150 and *Fmed* during the incubation period.

Solid-state NMR spectroscopy of wood samples in Petri plate assays

To study the impact of fungi and bacteria on wood degradation, we conducted ^{13}C CP/MAS NMR experiments on intact sterile sawdust (control) and sawdust inoculated with S150 alone, *Fmed* alone, and co-inoculated with S150 and *Fmed* (Fig. 3). The peaks observed in these experiments were assigned based on previous NMR studies on wood (Kolodziejski *et al.*, 1982; Haw *et al.*, 1984). Main chemical components of wood (cellulose, hemicellulose and lignin) were distinguished based on their characteristic ^{13}C chemical shifts, although for several regions (e.g. 65–80 ppm), signals overlap due to similar carbohydrate structures. Due to limited overlap in the 81–93 ppm region, the relative intensity of the two structural forms (crystalline and amorphous) of wood cellulose was compared. C-4 resonance of amorphous cellulose was observed at ~85 ppm, whereas crystalline cellulose resonance appeared at ~89 ppm (Park *et al.*, 2009). We derived the cellulose crystallinity index (Crl) by integrating the peaks of the crystalline and amorphous C-4 spectral area after deconvolution, following the procedure described in Davis *et al.* (1994). An increase in Crl (Fig. 3D) was observed in the sawdust inoculated with S150, changing from $17\% \pm 1\%$ for the control to $27\% \pm 1\%$ for that inoculated with S150. A similar effect was observed after inoculation with *Fmed*, with Crl increasing to $30\% \pm 1\%$. These results indicated that S150 and *Fmed* both had the ability to specifically degrade cellulose. The increase in Crl suggests that fungi and bacteria might have a preferential effect on amorphous cellulose, which is structurally easier to degrade compared to crystalline cellulose. As Crl is calculated as $\text{Crl} = a/a + b$, with a and b being the crystalline and amorphous contribution respectively, a decrease in amorphous cellulose would increase the Crl. Such changes in the relative amount of amorphous cellulose as a result of wood degradation caused by fungi and bacteria are in line with the findings of previous studies (Davis *et al.*, 1994) on Colorado blue spruce. When co-inoculated with S150 and *Fmed*, Crl further increased to $34\% \pm 1\%$, which corresponds to twice the Crl value obtained in the control sample, suggesting a synergistic effect of bacteria and fungi on cellulose degradation.

In addition to the preferential degradation of amorphous cellulose, the CPMAS spectra reveal an overall decrease in aromatic signals of lignin, especially the

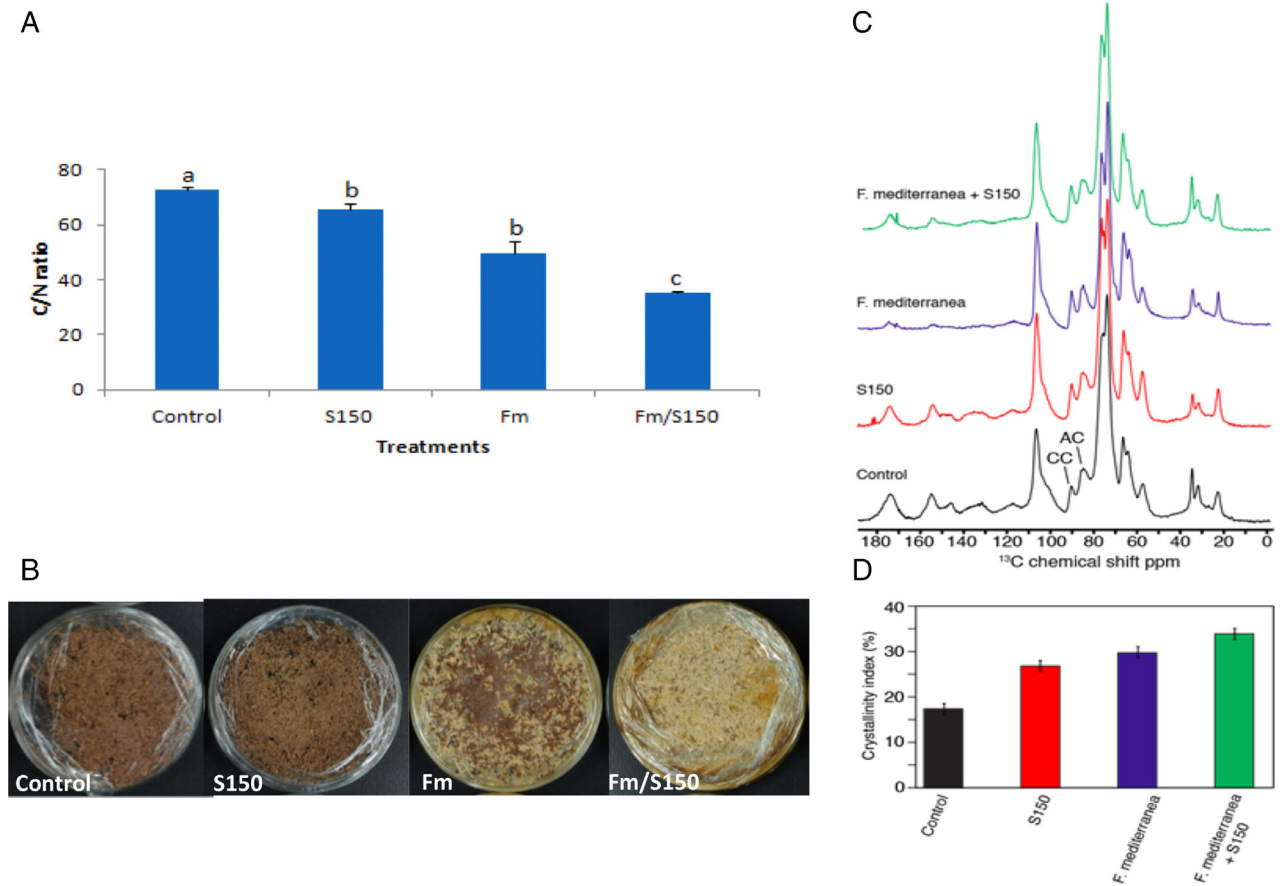


Fig. 3. Wood decay characterization after 8 months of incubation in Petri plates with *Fmed* (Fm) and *Paenibacillus* sp. (S150), alone or in combination, compared to a control without microorganisms.

A. C/N ratio, (B) Images of the different microcosmes give combinations at the end of experiments, (C) CPMAS ¹³C-detected spectra of sawdust samples (Solid-state NMR analysis) and (D) Crystallinity index (%) determined from the crystalline and amorphous contribution observed in NMR spectra. [Color figure can be viewed at wileyonlinelibrary.com]

guaiacyl C-1 and C-4 contribution at ~146 ppm, in the samples inoculated with *Fmed* and co-inoculated with *Fmed* and S150. This effect was not observed in sawdust inoculated only with S150, suggesting a stronger lignin-degrading effect of the fungus compared to that of the bacterium.

Genome analysis of S150

Genomic features and taxonomic affiliation. The genome of strain S150 was analyzed and was found to have a total size of 7.45 Mb, as well as an average G + C content of 52.54% (Table 2). The analysis based on 468 markers showed a genome completeness of 99.8% and contamination around 1.59%. The taxonomical analysis could not assign a species to the strain as it did not reach the required 95% ANI threshold for species circumscription. The genomic features of the strain are summarized in Table 2.

Table 2. Summary of the genomic feature of strain S150.

Feature	S150
Organism	<i>Paenibacillus</i> sp.
Length (bp)	74 15 460
Coverage	229.3607 ± 109.6652
Completeness (%)	99.47
GC content (%)	52.54
Contigs	102
Total genes	6,292
Predicted CDS	6,200
CRISPR number	6
rRNA number	6
tRNA number	85
tmRNA number	1

Genes predicted to be involved in carbohydrate metabolism. RAST annotation allowed the detection of several genes (230) involved in carbohydrate transport and metabolism, in addition to other clusters of orthologue groups. Seven genes involved in xylose (xyloside) degradation were detected (Table 3), namely, *XylIA* coding for a

Table 3. Protein encoding genes (part of the carbohydrate transport and metabolism) predicted to be involved in xylose (xylosides) degradation pathway of strain S150 determined by RAST.

Feature	Gene	Functional roles
Genes involved in xylose (xylosides) degradation pathway	<i>XylA</i>	Xylose isomerase (EC 5.3.1.5)
	<i>XylB</i>	Xylulose kinase (EC 2.7.1.17)
	<i>Xyl3</i>	Beta xylosidase (EC 3.2.1.37)
	<i>XynA</i>	Endo-1,4-beta-xylanase A precursor (EC 3.2.1.8)
	<i>XDH</i>	D-xylose 1-dehydrogenase (EC 1.1.1.175)
	<i>XL</i>	Xynolactone (EC 3.1.1.68)
	<i>XTD</i>	Xylonate dehydratase (EC 4.2.1.82)

xylose isomerase that catalyses the reaction of D-xylose to D-xylulose, *XylB* coding for a xylulose kinase that catalyses phosphorylation of D-xylulose to D-xylulose 5-phosphate, *Xyl3* coding for a beta-xylosidase and *XynA* coding for endo-1,4-beta-xylanase. A precursor that endohydrolyse (1→4)-beta-D-xylosidic linkages in xylans. *XDH* was also found that codes for a D-xylose 1 dehydrogenase (catalyses the reaction: D-xylose + NAD (+) ⇌ D-xylonolactone + NADH). Lastly, *XL* coding for a xynolactone (catalyses the reaction: D-xylono-1,4-lactone + H₂O ⇌ D-xylonate), and *XTD* coding for a xylonate dehydratase (catalyses the reaction: D-xylonate ⇌ 2-dehydro-3-deoxy-D-arabinonate + H₂O) were also detected (Table 3). Genes involved in the pentose-phosphate pathway were further analyzed. They code for transketolase, ribose-phosphate

pyrophosphokinase, glucose-6-phosphate 1-dehydrogenase, 6-phosphogluconolactonase, dehydrogenase, xylulose 5-phosphate, fructose 6-phosphate phosphoketolase and transaldolase (Table S1). No gene, possibly involved in lignin degradation (related to lignin-degrading auxiliary enzymes and lignin-modifying enzymes) was detected in the genome of S150 (Tables S1 and S2).

Furthermore, we also analyzed all gene clusters related to carbohydrate-active enzymes (CAZy) to have a better view of the functions of carbohydrate-related genes such as auxiliary activities, carbohydrate-binding modules and encoding carbohydrate esterases, glycoside hydrolases, glycosyltransferases and polysaccharide lyases (Figs 4–5). Among them, several GH families, as well as subfamilies, showed potential cellulase activities (i.e. endo β-1,4-glucanases) and activities on arabinofuranosides, fucosides, mannosides, xyloses and xylans (xylosides), and galactosides and glucuronides (Table S3).

Genes predicted to be involved in plant–microbe interaction. The carbohydrate metabolism of S150 and genes in its genome encoding polysaccharide lyases may be correlated to its behavior as an endophyte. In addition, the analysis of its genome also enabled the detection of genes encoding proteins that are predicted to be involved in plant–microbe interaction, including motility and chemotaxis, biofilm, siderophore and iron transport (Table S4), as well as genes related to oxidative stress and detoxification (Table S5). Interestingly, S150 also possesses genes involved in resisting copper and metalloids (Table S6) but not arsenic. However, a homologous

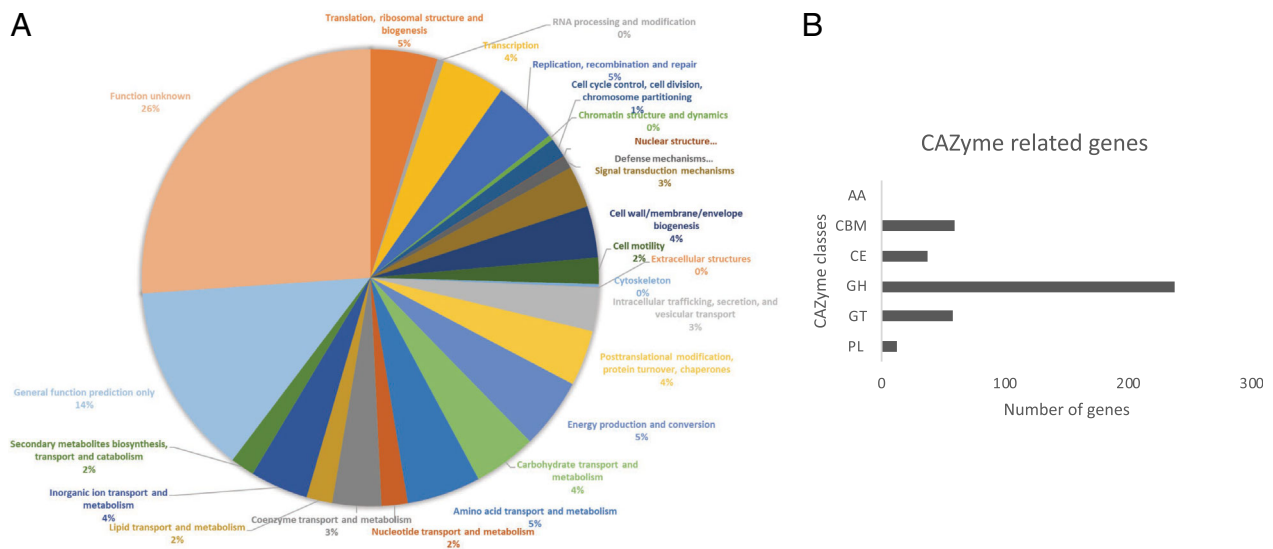


Fig. 4. (A) Cluster Orthologue Group (COG) categories of *Paenibacillus* sp. (S150), (B): Carbohydrate-active enzymes (CAZymes) related genes of strain S150. AA: auxiliary activities, CBM: carbohydrate-binding modules, CE: carbohydrate esterases, GH: Glycoside hydrolases, GT: Glycosyltransferases, PL: Polysaccharide lyases. [Color figure can be viewed at wileyonlinelibrary.com]

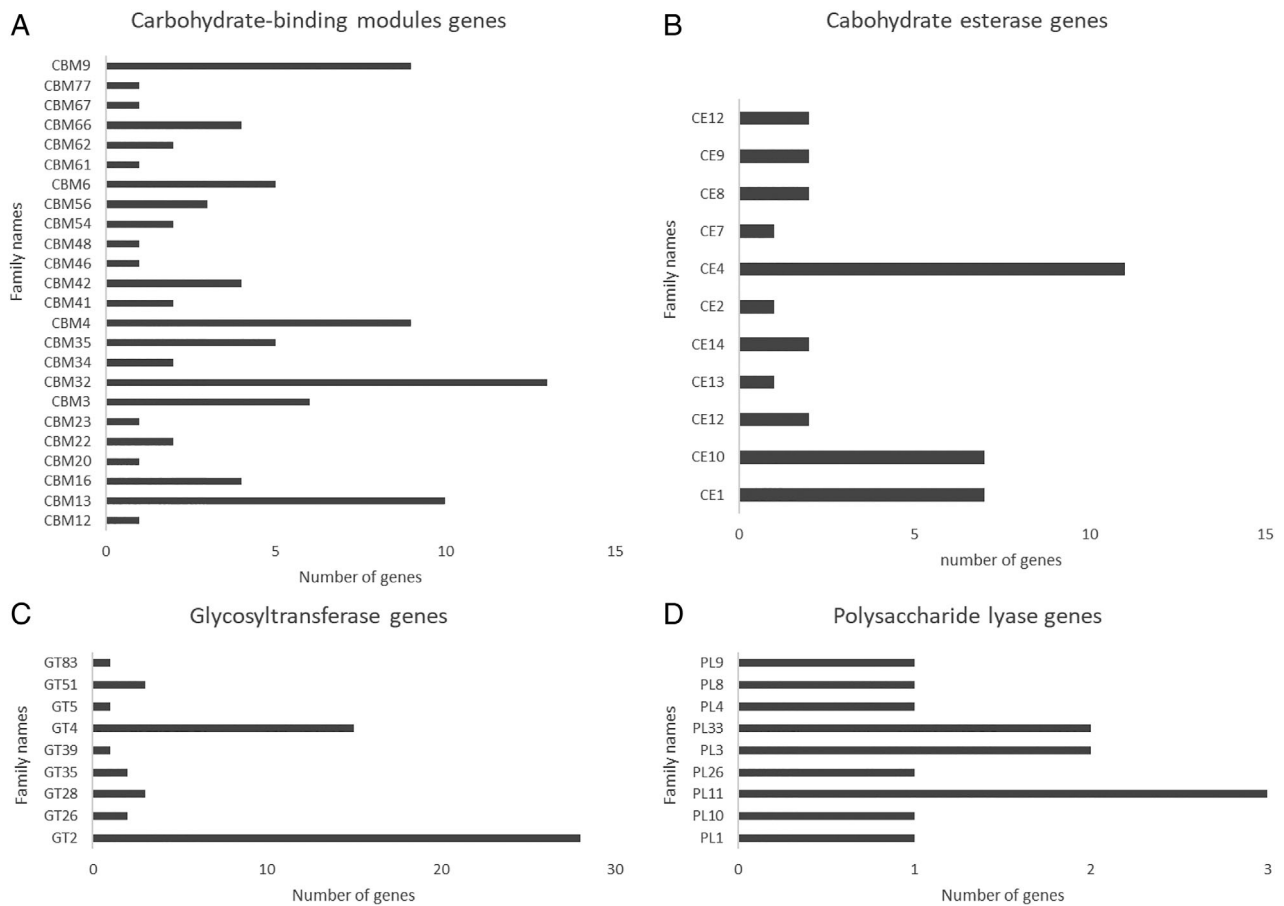


Fig. 5. Carbohydrate-active enzymes (CAZymes) related genes of strain S150 assessed with dbCAN2. CBM: carbohydrate-binding modules (A), CE: Carbohydrate esterases (B), GT: Glycosyltransferases (C), PL: Polysaccharide lyases (D).

gene of the repressor of the arsenic resistance operon was detected by eggNOG analysis (Table S2).

Genes predicted to be involved in fungal stimulation. Several gene clusters involved in the metabolism of vitamins such as thiamin (B1), riboflavin (B2), pyridoxin (B6), biotin (B7), folate (B9), cobalamin (B12), menaquinone (K1), phyloquinone (K2) and ubiquinone (Q10) were detected in S150 (Table S1). As per previous studies, these genes could be involved in fungal stimulation (del Barrio-Duque *et al.*, 2019, 2020). These studies showed several strains of *Proteobacteria* and *Mycobacteriaceae* promoting the growth of the mycorrhiza-like fungus *Serendipita indica*. Only a few genes reported to be involved in the provision of nitrogen to the fungus were identified (Table S1).

Biosynthetic gene clusters involved in secondary metabolite production. A total of six potential gene clusters involved in secondary metabolite production were identified. These clusters showed no similarity to genes encoding known compounds. However, one cluster

encoding a putative nonribosomal peptide synthetase (NRPS) showed 46% similarity to gene cluster responsible of bacillibactin (a catechol based siderophore), and another related to lasso peptide (synthesized and post-translationally modified peptides; RiPPs) showed 100% similarity to most similar known cluster related to paeninodin, which was proposed to serve as a signal molecule, and an antimicrobial and antiviral compound (Zhu *et al.*, 2016; Khurana *et al.*, 2020) (Fig. 6). The draft genome sequence of the strain is available at NCBI, BioProject PRJNA643435, with the DDBJ/ENA/GenBank accession number JACBYI000000000.

Discussion

Specifically adapted fungi and bacteria both have the ability to colonize grapevine wood tissues (Bruez *et al.*, 2014, 2015, 2020; Campisano *et al.*, 2014; Pinto *et al.*, 2014), but based on studies on GTD, fungi were almost exclusively considered responsible for wood degradation leading to necrosis (Larignon and Dubos, 1997; Mugnai *et al.*, 1999; Mostert *et al.*, 2006; Bertsch

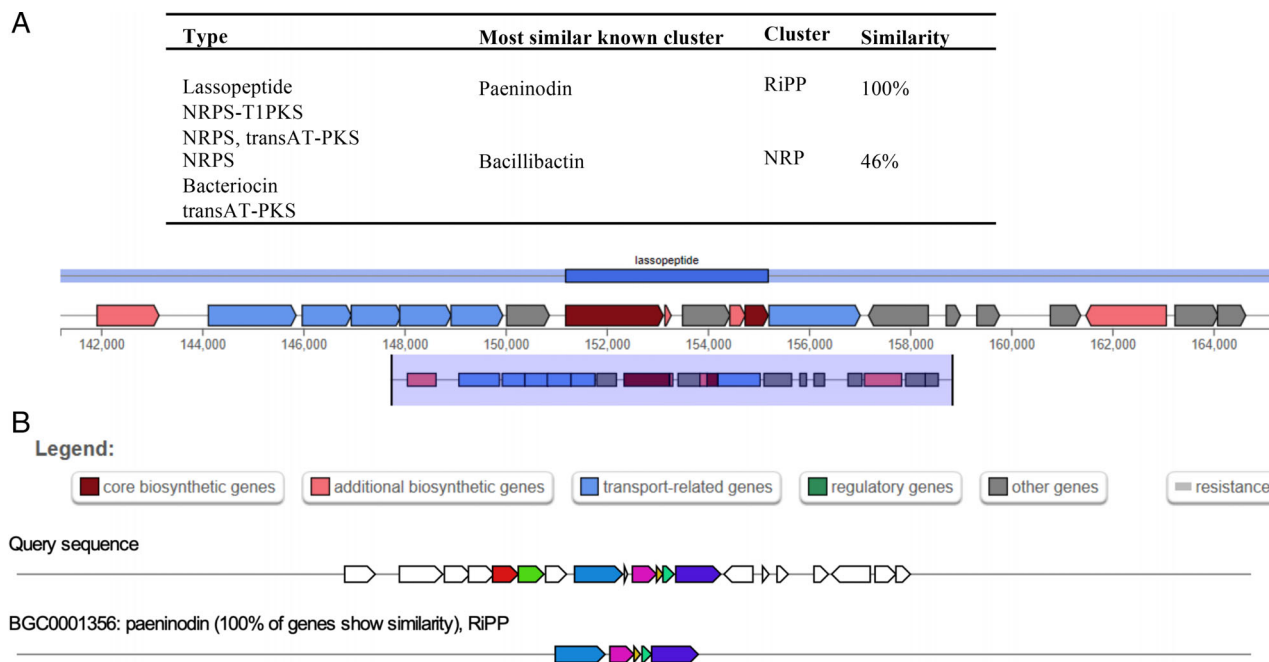


Fig. 6. Secondary metabolite prediction in strain S150 assessed with antiSMASH.

A. Type of cluster and most similar one.

B. Homologous gene cluster. [Color figure can be viewed at wileyonlinelibrary.com]

et al., 2013). In our study, we tested the hypothesis that synergistic interaction between a pathogenic GTD-fungus *Fmed* (a basidiomycete), and some bacterial strains inhabiting grapevine woods may have an important role in the wood-degradation process, increasing the overall level of degradation.

Bacteria colonizing wood grapevine

V5–V9 region of the 16S rRNA gene sequencing was used to identify the bacterial population colonizing the wood trunks and cordons of esca-symptomatic grapevines. These bacterial communities were dominated by members of the phyla *Proteobacteria* and *Firmicutes*. Among the nine families of *Proteobacteria*, *Xanthomonadaceae* was the most abundant. This is in accordance with prior findings in decaying wood of pine (Kielak *et al.*, 2016), beech (Valášková *et al.*, 2009), and in microcosms containing beech sawdust inoculated with *Phanerochaete chrysosporium* (Hervé *et al.*, 2014, 2016). It has also been reported that *Xanthomonadaceae* were able to degrade the lignocellulose (cellulose, hemicellulose and lignin) of different lignocellulose substrates under controlled conditions (Zimmermann, 1990; Behera *et al.*, 2014; Ceballos *et al.*, 2017; Oh *et al.*, 2017). At genus level, the isolated bacterial community was composed primarily of *Pseudomonas*, which aligns with previous results demonstrating this genus as the most

abundant in many organs as well as sap of grapevine (West *et al.*, 2010; Martins *et al.*, 2012, 2013; Faist *et al.*, 2016; Deyett *et al.*, 2017; Compant *et al.*, 2019; Deyett and Rolshausen, 2019). An association of *Xanthomonas* and *Pseudomonas* with wood decay processes of *Picea abies* was also reported (Probst *et al.*, 2018).

Bacterial and fungal degradation of wood components

In the present study, 59 bacterial strains obtained from various wood tissues, representing various taxa, were screened for their ability to degrade the three main components of wood, i.e. cellulose, hemicellulose and lignin, and their ability to inhibit *Fmed*. While 18 bacterial strains showed cellulolytic and xylanolytic activities, none of the bacterial strains was able to degrade lignin; conversely, the fungus *Fmed* specifically degraded lignin, as shown by CPMAS NMR analysis. Previous studies have also shown that there was no ligninolytic activity in bacterial strains isolated from spruce stumps or in microcosms containing beech sawdust (Murray and Woodward, 2007; Hervé *et al.*, 2016). For further investigations, we therefore selected *Paenibacillus* sp. strain S150, a bacterial strain able to degrade cellulose and hemicellulose, and did not inhibit *Fmed in vitro*. However, none of the selected *Xanthomonas* and *Pseudomonas* strains

(considered as associated with wood decay processes, as described above) has shown the last criteria.

By studying the physicochemical properties of wood-blocks exposed to *Fmed*, CPMAS NMR showed that *Fmed* preferentially degrades both lignin and amorphous cellulose. These results are consistent with the findings of a previous study (Bari *et al.*, 2015), which showed that after 120-days exposure of Oriental beech to the white-rot fungi *Pleurotus ostreatus* and *Trametes versicolor*, several properties of wood, such as its hardness, and cellulose and lignin content, declined.

Interaction between bacteria and fungi in wood degradation

Bacterial–fungal interaction involved in the wood degradation process has been reported before, but on other plants than grapevine (Hervé *et al.*, 2014, 2016; Kamei, 2017; Harry-asobara and Kamei, 2018). Evaluation of wood degradation was first done by measuring the C/N ratio of grapevine wood. This ratio provides information on changes in chemical composition of organic matter and thus reflects decomposition processes. The C/N ratio has already been identified as an important variable correlated to organic matter mass loss especially during the decomposition process (Eiland *et al.*, 2001; Lehmann *et al.*, 2002; Hervé *et al.*, 2014, 2016; Meriem *et al.*, 2016; Tramoy *et al.*, 2017). Our results demonstrated that when the two microorganisms were co-inoculated on grapevine sawdust, their interaction increased significantly grapevine wood degradation compared to that caused by the fungus alone and by the study of the physicochemical properties of wood by NMR. All results suggested a functional complementation of the two studied microorganisms.

Specific properties of the Paenibacillus strain S150

Several stains of *Paenibacillus*, isolated from diverse sources such as soil, bamboo leaves, decomposing rice straw and decaying woods, harbour enzymes that are involved in cellulose and xylan degradation (Nelson *et al.*, 2009; Khianggam *et al.*, 2011; Ghio *et al.*, 2012; Madhaiyan *et al.*, 2017). Our genome analysis of S150 revealed no gene involved in lignin degradation but several ones linked to cellulose, and xylose and xylan (xyloside) degradation. This point is of key importance since cellulose and hemicellulose represent up to 20%–35% of the ligno-cellulosic biomass of all plant cell walls (de Vries and Visser, 2001). The major hemicellulose in hardwood biomass is xylan (10%–35%), but it is less abundant in softwood (10%–15%). Xylan is made up of β -1,4-linked xylose residues with side branches of α -arabinofuranose and α -glucuronic acid (Balakshin *et al.*, 2011). We also found several genes responsible for vitamin metabolism that

could explain the increased *Fmed* growth observed in *in vitro* assays. Additionally, gene clusters involved in plant–microbe interaction were also identified.

Conclusions

In this study, we hypothesized that bacteria inhabiting grapevine wood could synergistically interact with an esca-causing pathogenic fungus, thus enhancing wood degradation. The obtained results confirmed this hypothesis and showed that (i) some bacteria can independently destructure wood components such as cellulose and hemicellulose, and (ii) fungal ability to degrade wood structures can be strongly influenced by some bacteria inhabiting wood. Specifically, the cellulolytic and xylanolytic strain S150 of the *Paenibacillus* sp. showed a synergistic interaction with the white-rot fungus *Fmed*. Having evidenced that fungus–bacteria synergistic interaction to promote wood degradation exists for microorganisms colonizing the wood of grapevines, the further step would be to point out its occurrence in mature grapevines and its role in the triggering and development of esca disease.

Experimental procedures

Grapevine material and sampling

Sampling was carried out in three 21-year-old vines of the cultivar Sauvignon blanc (*Vitis vinifera* L.) grafted onto the rootstock 101-14 MGt. The vines were located in an experimental vineyard near Bordeaux (INRAE, Villenave d'Ornon, France, 44°47'24.8"N, 0°34'35.1"W), planted in 2000. The vines had previously shown esca-foliar symptoms at least twice during a period of 4 years (2012–2016). The sampling method was as follows: plants were sectioned longitudinally to check the status of the wood tissues, i.e. necrotic or healthy, in the cordons and trunks. From the inner part of each organ, i.e. cordon and trunk, four types of wood tissues were sampled: necrotic (sectorial black streaks) tissues (NT), non-necrotic (apparently healthy) tissues (NNT), transition tissues between the necrotic and non-necrotic zones (TT) and white rot (decaying wood) tissues (WR), the typical necrotic tissue associated with esca (Maher *et al.*, 2012; Bruez *et al.*, 2015). A total of 24 samples, each consisting of 30 wood chips (around 5 mm in length), were collected corresponding to two organs (cordon and trunk) from three esca-symptomatic vines, and four tissues of each type (NT, NNT, TT and WR) were collected.

Wood-inhabiting bacterial strains

Isolation of bacteria from wood tissues of esca-symptomatic grapevines. The wood tissue samples were

surface-disinfected by immersing in 70% ethanol for 1 min and then in 2.5% calcium hypochlorite solution for 3 min. Then, the samples were rinsed thrice with sterile distilled water and dried on a sterile filter paper. The sterilized chips were plated onto three plates each of two different solid media [(five chips on each plate): R2A agar (Sigma-Aldrich)] amended with 100 mg L⁻¹ cycloheximide (Sigma) and nutrient agar (NA, Carl Roth) supplemented with 100 mg L⁻¹ cycloheximide, 10 mg L⁻¹ nalidixic acid and 5 g L⁻¹ glycerol. The plates were incubated at 28 °C for 48 h. A total of 237 bacterial strains were recovered from the 720 wood pieces collected (three symptomatic vines × two organs × four tissues × two media × five wood chips × three plates). After purification on Trypto-Casein-Soy Agar medium (TSA, Biokar Diagnostics) thrice, the strains were maintained at -20 °C on cryogenic storage beads (Viabank™, MWE, Wiltshire, England).

Identification by sequencing the partial 16S rRNA gene.

From the 237 bacterial strains that were recovered, genomic DNAs were extracted from pellets obtained after the centrifugation of pure cultures grown for 48 h in Tryptone-Soy Broth (TSB, Biokar) using the cetyltrimethylammonium bromide chloroform/isoamyl alcohol (24:1) protocol. DNA extracts were quantified using nanodrop (ND-1000, Thermo Scientific, Labtech) and then adjusted to a concentration of 20 ng µl⁻¹.

DNA samples were sent to Genewiz (Takeley, United Kingdom) for sequencing the 16S rRNA gene with the primers 799f (5'-AACMGGATTAGATACCCKG-3') and 1492r (5'-GTTACCTGTTACGACTT-3') (Heuer *et al.*, 1997; Redford *et al.*, 2010; Bruez *et al.*, 2015). For taxa level identification, sequences were compared with the GenBank database (nr/nt nucleotide collection using Megablast) using the BLASTn program (Altschul, 1997), with a >99% similarity cutoff. Sequences were then binned into taxa using the Muscle alignment method (Edgar, 2004) and the BioNJ distance-based phylogeny reconstruction algorithm (Gascuel, 1997) to select representative strains of each taxon for downstream analyses (microbiological functional analyses). A total of 59 taxa were defined. One bacterial strain of each taxon was selected for further analyses (Table 1).

Fmed strain and culture conditions

The *Fmed* isolate (Ph CO 36) used in this study was selected from the INRA-UMR 1065 SAVE collection (Bordeaux, France). This strain was originally obtained in 1996 in Saint Preuil, near Cognac, France. The strain was subcultured on Malt Agar medium (MA) and incubated at 27 °C (12 h light/12 h dark) for 7 days before being used in microcosm experimentations and 15 days

before being used in *in vitro* tests (confrontation and volatile tests).

Wood component decomposition by bacterial strains and Fmed

Selective media used. Three selective media were used for bacteria and *Fmed*. (i) Xylan medium: a medium containing xylan as the only carbon source [1 g L⁻¹ K₂HPO₄; 1 g L⁻¹ (NH₄)₂SO₄; 0.5 g L⁻¹ MgSO₄·7H₂O; 0.5 g L⁻¹ NaCl; 5 g L⁻¹ beechwood xylan (Apollo scientific); and 20 g L⁻¹ agar] (Hervé *et al.*, 2016); (ii) CMC medium: a medium containing carboxymethyl-cellulose as the sole carbon source [1 g L⁻¹ K₂HPO₄; 1 g L⁻¹ (NH₄)₂SO₄; 0.5 g L⁻¹ MgSO₄·7H₂O; 0.5 g L⁻¹ NaCl; 5 g L⁻¹ carboxymethyl-cellulose sodium salt (CMC, Sigma); and 20 g L⁻¹ agar] (Hervé *et al.*, 2016); (iii) RBBR medium: a Water Yeast Agar medium containing 0.05% RBBR (Sigma) [1 g L⁻¹ NaCl; 0.1 g L⁻¹ yeast extract (Difco); 1.95 g L⁻¹ MES (Sigma); and 20 g L⁻¹ agar; pH 5] (Hervé *et al.*, 2016). The laccase activity of *Fmed* was determined in Guaiacol medium: Potato Dextrose Agar (Biokar) medium containing 0.02% Guaiacol (Sigma).

Enzymatic assays. Petri plates containing the different selective media were inoculated with each pure microbial strain (59 selected bacteria and *Fmed*) and then incubated at 28 °C for 7 days in the dark. Four plates were replicated for each medium and strain. Lignolysis was indicated by the RBBR medium that turns from blue to pale pink when positive (Murray and Woodward, 2007). The xylanolytic activity on xylan medium and cellulolytic activity on CMC medium were detected using 0.1% Congo red (Sigma) staining for 40 min followed by washing with 1 M NaCl for counterstaining. Each enzymatic activity was measured based on the size (mm) of the clearing/discoloration zones formed around the bacterial or fungal colonies. The production of laccase by *Fmed* was indicated by the medium turning brown.

In vitro bacteria-Fmed co-cultures

Direct confrontation assays. A mycelial plug of *Fmed* (4 mm in diameter) was placed at the centre of MA plates, and after a week of incubation at 25 °C, selected bacterial strains were streaked at the edge of each plate. A set of plates was inoculated with the pathogen only. Three replicates were performed for each combination (bacterial strain/*Fmed*) tested. The plates were then incubated in the dark at 27 °C. After 1 week, the radial mycelial growth of *Fmed* was assessed by measuring the radius of the colony in mm (in the direction of the bacterial strain and also in the opposite direction). The mycelial growth inhibition percentage (GI%) was calculated using

the following equation: $GI\% = 100 \times (R2 - R1)/R2$, where R1 is the radial distance (mm) grown by *Fmed* in the direction of the bacterial strain, and R2 is the radial distance (mm) grown by the *Fmed* in the opposite direction.

Assay of the volatile substances produced by the bacteria. The *Fmed* strain was grown on MA plates for 7 days at 27 °C in the dark, and the bacterial strains were grown on TSA for 24 h at 28 °C. The bottoms of the plates were then placed face-to-face, with the bacterial culture plate placed below the *Fmed* plate, and sealed with Parafilm. This arrangement prevented physical contact between the two microorganisms. Plates were incubated at 27 °C in the dark for 7 days. The control plates consisted of *Fmed* plates inverted over sterile TSA medium. Three replicates were made for each bacterial strain and the control. The diameters of the fungal colonies were measured after 7 days of incubation, and the mycelial growth inhibition was calculated with respect to the control.

Microcosm experimentations

Degradation of lignin by *Fmed* • Experimental design. Grapevine cuttings of cv. Cabernet Sauvignon originating from INRA experimental vineyards near Bordeaux (Villenave d'Ormon, France, 44°47'24.8"N, 0°34'35.1"W) were used for the microcosm experimentations. After having removed the bark, wooden rods (30 mm in length, 10 mm in width) were sectioned and sterilized twice for 20 min at 120 °C, in a 2-day interval. Hundred microcosms were then prepared in Petri plates, each containing one wooden rod and a 7-day-old *Fmed* colony. Twenty controls were prepared with wooden rods incubated on sterile MA medium. The microcosms were sealed with Parafilm before being incubated for 2, 7 and 10 months at 25 °C in the dark.

- **Lignin content measurement in wooden rods by the determination of Klason lignin.** The lignin content following a short (2 months) and a long (7 and 10 months) exposure time to *Fmed* was determined using the Klason method (Kirk and Obst, 1988; Tláskal *et al.*, 2017).

The lignin content in control rods was also determined. Five replicate rods were used for each exposure time. All assays were performed twice.

Effect of bacteria–*Fmed* co-cultures on wood degradation • Selected bacteria and bacterial inocula. For inoculation, the bacterial strain S150 was prepared as described by Kamei (2017), with slight modifications. Liquid cultures were obtained by inoculating Erlenmeyer flasks containing TSB, with bacterial colonies previously grown on TSA and by incubating them at 27 °C for 24 h

using an orbital shaker at 150 rpm. Liquid cultures were then centrifuged twice at 5000 rpm for 10 min, and the pellets were resuspended in sterile water. Bacterial suspensions were quantified by fluorochrome staining (500 µl Chemsol B16 buffer + 2.5 µl Chemchrome V6 fluorescein acetate; Biomérieux, France) followed by epifluorescent direct counts using an optical microscope (Model BH2, Olympus, France). A minimum of 300 cells was counted in at least 10 different fields of view, and the average number of fluorescent cells per field was expressed as CFU ml⁻¹. The bacterial concentrations obtained were estimated at 10⁷ and 2 × 10⁷ CFU ml⁻¹.

- **Experimental design.** Two types of microcosms (in Erlenmeyer flasks and in Petri plates) were used to study the effect of S150 on wood degradation by *Fmed*.

- **Erlenmeyer flask microcosms.** Experimentations were carried out in 50 ml Erlenmeyer flasks sealed with adhesive tape containing 0.4 g of sterile sawdust wood (cv. Cabernet Sauvignon) sieved (mesh size 2 mm) and autoclaved twice, 2 days apart (for 20 min, at 120 °C). A mycelial disk (5 mm in diameter) taken from the margin of a 15-day-old colony, was then placed on sawdust already inoculated with 400 µl of bacterial cell suspension. Control flasks were inoculated with 400 µl of sterile distilled water. Each flask was sealed with a transparent adhesive tape and then incubated for 60 days at 28 °C in the dark.

Four treatments with three replicates each were tested: (i) controls containing sawdust with sterile water; (ii) *Fmed* with sterile water; (iii) *Fmed* and S150; and (iv) S150.

- **Petri plate microcosms.** Experimentations were carried out with the strain S150 in 90 mm Petri plates containing 2 g of sterile sawdust wood (*Vitis vinifera* L), sealed with adhesive tape. Grapevine sawdust was sieved (2 mm mesh) and autoclaved (for 20 min, at 120 °C) twice, with an interval of 2 days in between. Fungal inocula were prepared on grapevine wood rods as described in Section 6.1.1 of this text.

Wooden rods (1 cm long) were colonized with *Fmed* for 5 months, then placed on sawdust and inoculated with 5 ml of bacterial cell suspension. Control flasks were inoculated with 5 ml of sterile distilled water. Each Petri plate was sealed with transparent adhesive tape and incubated for 8 months at 28 °C in the dark.

- **Assessment of wood degradation • Measurement of C and N concentrations.** After incubation, the C and N contents of the woods were measured, in three repetitions of each modality, by the Dumas' method using a VarioMax cube elemental analyser at the USRAVE

precincts (USRAVE, INRAE Aquitaine, France). Size and color of the sawdust particles were observed for all assays.

- Solid-state NMR spectroscopy for analysis of the woods. The evaluation of wood components' degradation in Petri plate microcosms was carried out by using solid-state NMR (ssNMR), performed under magic-angle spinning (MAS) conditions. MAS ssNMR experiments were conducted on a 300 MHz spectrometer (Bruker Avance III) equipped with a double resonance 4 mm DVT MAS probe. MAS frequency was set to 11 kHz. ^{13}C -detected experiments were performed using a ^1H - ^{13}C cross-polarization (CP) transfer using a contact time of 500 μs , a recycle delay of 2 s, and 100 kHz proton decoupling during acquisition. 20 k scans were used per CPMAS experiment.

Cellulose crystallinity, measured as the crystallinity index (CrI), was calculated from the area of the (a) crystalline (87–93 ppm) and (b) amorphous (81–88 ppm) cellulose C4 signals, by deconvolution using a Lorentzian line shape.

Genome of Paenibacillus sp. strain S150

The bacterial genomic DNA was extracted following a phenol-chloroform based protocol after growing the strain in liquid TSB medium for 3 days and harvesting by centrifugation at 6000 rpm for 3 min. The bacterial pellet was resuspended in a lysis buffer (0.2 mg ml⁻¹ Proteinase K, 50 mM Tris-Cl, 1% SDS, 5 mM EDTA at pH 8 and 0.5 M NaCl) and incubated overnight (at 65 °C; 400 rpm). DNA was extracted twice using phenol–chloroform–isoamylalcohol at a ratio of 25:24:1 and collected by centrifugation at 6,000 rpm for 3 min as described in a previous study (del Barrio-Duque *et al.*, 2020). Genomic DNA was then purified with Amicon Ultra 0.5 ml 30K Centrifugal Filter Units (Millipore, Cork, Ireland) and resuspended in distilled sterile water. Whole-genome shotgun sequencing was performed on an Illumina NovaSeq 6000 mode S2 (GATC Biotech, Konstanz, Germany), producing approximately 6.2 million paired-end reads of 150 bp. The Illumina reads were then screened for the presence of PhiX using Bowtie 2 (v2.3.4.3) (Langmead and Salzberg, 2012); adapters were trimmed and quality filtering was accomplished with FASTP (v0.19.5) (Chen *et al.*, 2018). Sequence length distribution and quality were checked via FastQC (Andrews, 2010). Genome assembly was performed with SPAdes v3.13.0 (Bankevich *et al.*, 2012), and low-abundant (<2 \times) and short (<500 bp) contigs were discarded. Contigs were roughly checked for the presence of contaminants using BlobTools v1.1.1. The quality of genome assembly was determined using QualiMap v2.2 (Okonechnikov *et al.*, 2015) and QUASt v5.0.0 (Gurevich *et al.*, 2013),

and then genome completeness of the reconstructed genome was evaluated using CheckM v1.0.18 (Parks *et al.*, 2015). Gene annotation was carried out using Prokka v1.12 (Seemann, 2014) and NCBI Prokaryotic Genome Annotation Pipeline (PGAP). The presence of plasmids was ascertained by using Mash v2.1 against the PLSDB database (Galata *et al.*, 2019). Putative plasmid contigs were screened for the presence of genes coding for replication initiator proteins, *repA*. For this purpose, a curated FASTA file with ~8,000 *repA* genes was generated from plasmid genome sequences in NCBI. These *repA* gene sequences were used to build a database against which the selected contigs were aligned using BLAST+ v.2.10.0. These *repA* gene sequences were used to build a database against which the selected contigs were BLASTed. Functional annotation was performed using the ClassicRAST (Rapid Annotation using Subsystem Technology) webserver (<http://rast.nmpdr.org>) (Aziz *et al.*, 2008), and the hierarchical orthology framework EggNOG 4.5 (Huerta-Cepas *et al.*, 2016). CAZy families were ascertained with dbCAN2 based on the HMMER database. Annotation of proteins was based on the CAZy database (Lombard *et al.*, 2014). Biosynthetic gene clusters and secondary metabolites were further predicted using antiSMASH version 4.0.2 (Weber *et al.*, 2015). To assign objective taxonomic classifications to the genome, the software toolkit GTDB-Tk v0.3.2 was used (Parks *et al.*, 2018; Chaumeil *et al.*, 2020).

Statistical analyses

The experimental data obtained from *in vitro* or microcosm assays were compared using an analysis of variance (ANOVA) followed by Newman–Keuls' test ($P \leq 0.05$). These analyses were carried out with the StatBox software (Version 6.6, Grimmer[®] Logiciels, Paris).

Acknowledgments

This work was supported by the Industrial Chair GTD free funded by ANR (French National Research Agency) and the Hennessy Company to PR. CIVB (grant N°50689 to AS and AL), and the ERC Starting Grant no. 639020 to AL. SC received funding via DaFNE Project Nr. 101384 from the Austrian Federal Ministry for Sustainability and Tourism (BMNT). We are grateful to B. Nikolic from AIT Austrian Institute of Technology for DNA isolation of strain S150.

References

Altschul, S. (1997) Gapped BLAST and PSI-BLAST: a new generation of protein database search programs. *Nucleic Acids Res* **25**: 3389–3402.

- Andrews, S. (2010) FastQC: a quality control tool for high throughput sequence data. URL <http://www.bioinformatics.babraham.ac.uk/projects/fastqc>.
- Aziz, R.K., Bartels, D., Best, A.A., DeJongh, M., Disz, T., Edwards, R.A., *et al.* (2008) The RAST server: rapid annotations using subsystems technology. *BMC Genomics* **9**: 75.
- Balakshin, M., Capanema, E., Gracz, H., Chang, H., and Jameel, H. (2011) Quantification of lignin-carbohydrate linkages with high-resolution NMR spectroscopy. *Planta* **233**: 1097–1110.
- Bankevich, A., Nurk, S., Antipov, D., Gurevich, A.A., Dvorkin, M., Kulikov, A.S., *et al.* (2012) SPAdes: a new genome assembly algorithm and its applications to single-cell sequencing. *J Comput Biol* **19**: 455–477.
- Bari, E., Schmidt, O., and Oladi, R. (2015) A histological investigation of oriental beech wood decayed by *Pleurotus ostreatus* and *Trametes versicolor*. *For Pathol* **45**: 349–357.
- Behera, B.C., Parida, S., Dutta, S.K., and Thatoi, H.N. (2014) Isolation and identification of cellulose degrading bacteria from mangrove soil of mahanadi river delta and their cellulase production ability. *Am J Microbiol Res* **1**: 41–46.
- Bertsch, C., Ramírez-Suero, M., Magnin-Robert, M., Larignon, P., Chong, J., Abou-Mansour, E., *et al.* (2013) Grapevine trunk diseases: complex and still poorly understood. *Plant Pathol* **62**: 243–265. <https://doi.org/10.1111/j.1365-3059.2012.02674.x>.
- Boer, W., Folman, L.B., Summerbell, R.C., and Boddy, L. (2005) Living in a fungal world: impact of fungi on soil bacterial niche development. *FEMS Microbiol Rev* **29**: 795–811.
- Brown, A.A., Lawrence, D.P., and Baumgartner, K. (2020) Role of basidiomycete fungi in the grapevine trunk disease esca. *Plant Pathol* **69**: 205–220. <https://doi.org/10.1111/ppa.13116>.
- Bruez, E., Haidar, R., Alou, M.T., Vallance, J., Bertsch, C., Mazet, F., *et al.* (2015) Bacteria in a wood fungal disease: characterization of bacterial communities in wood tissues of esca-foliar symptomatic and asymptomatic grapevines. *Front Microbiol* **6**: 1137.
- Bruez, E., Vallance, J., Gautier, A., Laval, V., Compant, S., Maurer, W., *et al.* (2020) Major changes in grapevine wood microbiota are associated with the onset of esca, a devastating trunk disease. *Environ Microbiol* **22**: 5189–5206.
- Bruez, E., Vallance, J., Gerbore, J., Lecomte, P., Da Costa, J.P., Guerin-Dubrana, L., and Rey, P. (2014) Analyses of the temporal dynamics of fungal communities colonizing the healthy wood tissues of Esca leaf-symptomatic and asymptomatic vines. *PLoS One* **9**: e95928.
- Calzarano, F., Cichelli, A., and Odoardi, M. (2001) Preliminary evaluation of variations in composition induced by esca on cv. Trebbiano d'Abruzzo grapes and wines. *Phytopathol Mediterr* **40**: S443–S448.
- Calzarano, F., Seghetti, L., Del, C., and Cichelli, A. (2004) Effect of Esca on the quality of berries, musts and wines. *Phytopathol Mediterr* **43**: 125–135.
- Campisano, A., Antonielli, L., Pancher, M., Yousaf, S., Pindo, M., and Pertot, I. (2014) Bacterial endophytic communities in the grapevine depend on pest management. *PLoS One* **9**: e112763.
- Ceballos, S.J., Yu, C., Claypool, J.T., Singer, S.W., Simmons, B.A., Thelen, M.P., *et al.* (2017) Development and characterization of a thermophilic, lignin degrading microbe. *Process Biochem* **63**: 193–203. <https://doi.org/10.1016/j.procbio.2017.08.018>.
- Chaumeil, P.A., Mussig, A.J., Hugenholtz, P., and Parks, D. H. (2019) GTDB-Tk: a toolkit to classify genomes with the Genome Taxonomy Database. *Bioinformatics* **36**: 1925–1927.
- Chen, S., Zhou, Y., Chen, Y., and Gu, J. (2018) fastp: an ultra-fast all-in-one FASTQ preprocessor. *Bioinformatics* **34**: i884–i890.
- Cholet, C., Bruez, E., Lecomte, P., Barsacq, A., Martignon, T., Giudici, M., *et al.* (2021) Plant resilience and physiological modifications induced by curettage of Esca-diseased grapevines. *OENO One* **55**: 153–169. <https://doi.org/10.20870/oenone.2021.55.1.4478>.
- Clausen, C.A. (1996) Bacterial associations with decaying wood: a review. *Int Biodeter Biodegr* **37**: 101–107.
- Cloete, M., Fischer, M., Mostert, L., and Halleen, F. (2014) A novel *Fomitiporia* species associated with esca on grapevine in South Africa. *Mycol Progress* **13**: 303–311. <https://doi.org/10.1007/s11557-013-0915-5>.
- Compant, S., Samad, A., Faist, H., and Sessitsch, A. (2019) A review on the plant microbiome: ecology, functions, and emerging trends in microbial application. *J Adv Res* **19**: 29–37.
- Cornelissen, J.H.C., Sass-Klaassen, U., Poorter, L., van Geffen, K., van Logtestijn, R.S.P., van Hal, J., *et al.* (2012) Controls on coarse wood decay in temperate tree species: birth of the LOGLIFE experiment. *Ambio* **41**: 231–245.
- Davis, M.F., Schroeder, H.R., and Maciel, G.E. (1994) Solid-state ¹³C nuclear magnetic resonance studies of wood decay. I. White rot decay of colorado Blue Spruce. *Holzforschung* **48**: 99–105. <https://doi.org/10.1515/hfsg.1994.48.2.99>.
- de Vries, R.P., and Visser, J. (2001) Aspergillus enzymes involved in degradation of plant cell wall polysaccharides. *Microbiol Mol Biol Rev* **65**: 497–522.
- del Barrio-Duque, A., Ley, J., Samad, A., Antonielli, L., Sessitsch, A., and Compant, S. (2019) Beneficial endophytic bacteria-*Serendipita indica* interaction for crop enhancement and resistance to phytopathogens. *Front Microbiol* **10**: 2888.
- del Barrio-Duque, A., Samad, A., Nybroe, O., Antonielli, L., Sessitsch, A., and Compant, S. (2020) Interaction between endophytic Proteobacteria strains and *Serendipita indica* enhances biocontrol activity against fungal pathogens. *Plant Soil* **451**: 277–305. <https://doi.org/10.1007/s11104-020-04512-5>.
- Deyett, E., and Rolshausen, P.E. (2019) Temporal dynamics of the sap microbiome of grapevine under high pierce's disease pressure. *Front Plant Sci* **10**: 1246.
- Deyett, E., Roper, M.C., Ruegger, P., Yang, J.I., Borneman, J., and Rolshausen, P.E. (2017) Microbial landscape of the grapevine endosphere in the context of

- Pierce's disease. *Phytobiomes J* **1**: 138–149. <https://doi.org/10.1094/PBIOMES-08-17-0033-R>.
- Edgar, R.C. (2004) MUSCLE: multiple sequence alignment with high accuracy and high throughput. *Nucleic Acids Res* **32**: 1792–1797.
- Eiland, F., Klamer, M., Lind, A.M., Leth, M., and Bååth, E. (2001) Influence of initial C/N ratio on chemical and microbial composition during long term composting of straw. *Microb Ecol* **3**: 272–280.
- Faist, H., Keller, A., Hentschel, U., and Deeken, R. (2016) Grapevine (*Vitis vinifera*) crown galls host distinct microbiota. *Appl Environ Microbiol* **82**: 5542–5552.
- Fischer, M. (2000) Grapevine wood decay and lignicolous basidiomycetes. *Phytopathol Mediterr* **39**: 100–106.
- Fischer, M. (2002) A new wood-decaying basidiomycete species associated with esca of grapevine: *Fomitiporia mediterranea* (Hymenochaetales). *Mycol Progress* **1**: 314–324. <https://doi.org/10.1007/s11557-006-0029-4>.
- Fischer, M. (2006) Biodiversity and geographic distribution of basidiomycetes causing esca-associated white rot in grapevine: a worldwide perspective. *Phytopathol Mediterr* **45**: S30–S42.
- Fischer, M., and González Garcia, V. (2015) An annotated checklist of European basidiomycetes related to white rot of grapevine (*Vitis vinifera*). *Phytopathol Mediterr* **54**: 281–298.
- Fourie, P.H., Halleen, F., van der Vyver, J., and Schreuder, W. (2001) Effect of *Trichoderma* treatments on the occurrence of decline pathogens in the roots and rootstocks of nursery grapevines. *Phytopathol Mediterr* **40**: S473–S478.
- Galata, V., Fehlmann, T., Backes, C., and Keller, A. (2019) PLSDb: a resource of complete bacterial plasmids. *Nucleic Acids Res* **47**: D195–D202.
- Gascuel, O. (1997) BIONJ: an improved version of the NJ algorithm based on a simple model of sequence data. *Mol Biol Evol* **14**: 685–695.
- Ghio, S., Lorenzo, G.S.D., Lia, V., Talia, P., Cataldi, A., Grasso, D., and Campos, E. (2012) Isolation of *Paenibacillus* sp. and *Variovorax* sp. strains from decaying woods and characterization of their potential for cellulose deconstruction. *Int J Biochem* **3**: 352–364.
- Gurevich, A., Saveliev, V., Vyahhi, N., and Tesler, G. (2013) QUAST: quality assessment tool for genome assemblies. *Bioinformatics* **29**: 1072–1075.
- Haidar, R., Deschamps, A., Roudet, J., Calvo-Garrido, C., Bruez, E., Rey, P., and Fermaud, M. (2016a) Multi-organ screening of efficient bacterial control agents against two major pathogens of grapevine. *Biol Control* **92**: 55–65. <https://doi.org/10.1016/j.biocontrol.2015.09.003>.
- Haidar, R., Roudet, J., Bonnard, O., Dufour, M.C., Corio-Costet, M.F., Fert, M., et al. (2016b) Screening and modes of action of antagonistic bacteria to control the fungal pathogen *Phaeoaniella chlamydospora* involved in grapevine trunk diseases. *Microbiol Res* **192**: 172–184.
- Haidar, R., Yacoub, A., Pinard, A., Roudet, J., Fermaud, M., and Rey, P. (2020) Synergistic effects of water deficit and wood-inhabiting bacteria on pathogenicity of *Neofusicoccum parvum*, a major grapevine trunk pathogen. *Phytopathol Mediterr* **59**: 81–93.
- Harry-asobara, J.L., and Kamei, I. (2018) Bacterial strains isolated from cedar wood improve the mycelial growth and morphology of white rot fungus *Phlebia brevispora* on agar and liquid medium. *J Wood Sci* **64**: 444–450. <https://doi.org/10.1007/s10086-018-1723-y>.
- Haw, J.F., Maciel, G.E., and Schroeder, H.A. (1984) Carbon-13 nuclear magnetic resonance spectrometric study of wood and wood pulping with cross polarization and magic-angle spinning. *Anal Chem* **56**: 1323–1329.
- Hervé, V., Ketter, E., Pierrat, J.-C., Gelhay, E., and Frey-Klett, P. (2016) Impact of *Phanerochaete chrysosporium* on the functional diversity of bacterial communities associated with decaying wood. *PLoS One* **11**: e0147100.
- Hervé, V., Le Roux, X., Uroz, S., Gelhay, E., and Frey-Klett, P. (2014) Diversity and structure of bacterial communities associated with *Phanerochaete chrysosporium* during wood decay: bacteria of the white-rot mycosphere. *Environ Microbiol* **16**: 2238–2252.
- Heuer, H., Krsek, M., Baker, P., Smalla, K., and Wellington, E.M. (1997) Analysis of actinomycete communities by specific amplification of genes encoding 16S rRNA and gel-electrophoretic separation in denaturing gradients. *Appl Environ Microbiol* **63**: 3233–3241.
- Huerta-Cepas, J., Szklarczyk, D., Forslund, K., Cook, H., Heller, D., Walter, M.C., et al. (2016) eggNOG 4.5: a hierarchical orthology framework with improved functional annotations for eukaryotic, prokaryotic and viral sequences. *Nucleic Acids Res* **44**: D286–D293.
- Kamei, I. (2017) Co-culturing effects of coexisting bacteria on wood degradation by *Trametes versicolor*. *Curr Microbiol* **74**: 125–131.
- Khiangnam, S., Tanasupawat, S., Akarachanya, A., Kim, K.K., Lee, K.C., and Lee, J.S. (2011) *Paenibacillus xylanisolvans* sp. nov., a xylan-degrading bacterium from soil. *Int J Syst Evol Microbiol* **61**: 160–164.
- Khurana, H., Sharma, M., Verma, H., Lopes, B.S., Lal, R., and Negi, R.K. (2020) Genomic insights into the phylogeny of *Bacillus* strains and elucidation of their secondary metabolic potential. *Genomics* **112**: 3191–3200.
- Kielak, A.M., Scheublin, T.R., Mendes, L.W., van Veen, J.A., and Kuramae, E.E. (2016) Bacterial community succession in pine-wood decomposition. *Front Microbiol* **7**: 231.
- Kirk, T.K., and Obst, J.R. (1988) Lignin determination. In *Methods in Enzymology*, Wood, W.A., and Kellogg, S.T. (eds). New York: Academic Press, pp. 87–101. [https://doi.org/10.1016/0076-6879\(88\)61014-7](https://doi.org/10.1016/0076-6879(88)61014-7).
- Kolodziejski, W., Frye, J.S., and Maciel, G.E. (1982) Carbon-13 nuclear magnetic resonance spectrometry with cross polarization and magic-angle spinning for analysis of lodgepole pine wood. *Anal Chem* **54**: 1419–1424.
- Kraus, C., Voegelé, R.T., and Fischer, M. (2019) Temporal development of the culturable, endophytic fungal community in healthy grapevine branches and occurrence of GTD-associated fungi. *Microb Ecol* **77**: 866–876.
- Langmead, B., and Salzberg, S.L. (2012) Fast gapped-read alignment with Bowtie 2. *Nat Methods* **9**: 357–359.
- Larignon, P., and Dubos, B. (1997) Fungi associated with Esca disease in grapevine. *Eur J Plant Pathol* **103**: 147–157. <https://doi.org/10.1023/A:1008638409410>.
- Laveau, C., Letouze, A., Louvet, G., Bastien, S., and Guerin-Dubrana, L. (2009) Differential aggressiveness of fungi

- implicated in esca and associated diseases of grapevine in France. *Phytopathol Mediterr* **48**: 32–46.
- Lehmann, M.F., Bernasconi, S.M., Barbieri, A., and McKenzie, J.A. (2002) Preservation of organic matter and alteration of its carbon and nitrogen isotope composition during simulated and in situ early sedimentary diagenesis. *Geochim Cosmochim Acta* **66**: 3573–3584. [https://doi.org/10.1016/S0016-7037\(02\)00968-7](https://doi.org/10.1016/S0016-7037(02)00968-7).
- Lladó, S., López-Mondéjar, R., and Baldrian, P. (2017) Forest soil bacteria: diversity, involvement in ecosystem processes, and response to global change. *Microbiol Mol Biol Rev* **81**: e00063-16.
- Lombard, V., Golaconda Ramulu, H., Drula, E., Coutinho, P. M., and Henrissat, B. (2014) The carbohydrate-active enzymes database (CAZy) in 2013. *Nucleic Acids Res* **42**: D490–D495.
- Madhaiyan, M., Poonguzhali, S., Saravanan, V.S., Duraipandian, V., Al-Dhabi, N.A., Kwon, S.W., and Whitman, W.B. (2017) *Paenibacillus polysaccharolyticus* sp. nov., a xylanolytic and cellulolytic bacteria isolated from leaves of bamboo *Phyllostachys aureosulcata*. *Int J Syst Evol Microbiol* **67**: 2127–2133.
- Maher, N., Piot, J., Bastien, S., Vallance, J., Rey, P., and Guérin-Dubrana, L. (2012) Wood necrosis in esca-affected vines: types, relationships and possible links with foliar symptom expression. *J Int Sci Vigne Vin* **46**: 15–27.
- Marraschi, R., Ferreira, A.B.M., da Silva Bueno, R.N., Leite, J.A.B.P., Lucon, C.M.M., Harakava, R., et al. (2018) A protocol for selection of *Trichoderma* spp. to protect grapevine pruning wounds against *Lasiodiplodia theobromae*. *Braz J Microbiol* **50**: 213–221.
- Martins, G., Miot-Sertier, C., Lauga, B., Claisse, O., Lonvaud-Funel, A., Soulas, G., and Masneuf-Pomarède, I. (2012) Grape berry bacterial microbiota: impact of the ripening process and the farming system. *Int J Food Microbiol* **158**: 93–100.
- Martins, G., de Lauga, B., de Mercier, A., de Lonvaud, A., and Soulas, M.L. (2013) Characterization of epiphytic bacterial communities from grapes, leaves, bark and soil of grapevine plants grown, and their relations. *PLoS ONE* **8**: e73013. <https://doi.org/10.1371/journal.pone.0073013>.
- Meriem, S., Tjitrosoedirjo, S., Kotowska, M., Hertel, D., and Triadiati, T. (2016) Carbon and nitrogen stocks in dead wood of tropical lowland forests as dependent on wood decay stages and land-use intensity. *Ann For Res* **59**: 299–310.
- Mirabolfathy, M., Hosseinian, L., and Peighami Ashnaei, S. (2021) Fungal communities of grapevine decline in the main grape-growing regions of Iran. *Indian Phytopathol*. 1–7. <https://doi.org/10.1007/s42360-020-00314-y>.
- Mostert, L., Groenewald, J.Z., Gams, W., Summerbell, R., and Crous, P.W. (2006) Taxonomy and pathology of *Togninia* (*Diaporthales*) and its *Phaeoacremonium* anamorphs. *Stud Mycol* **54**: 1–115.
- Mugnai, L., Graniti, A., and Surico, G. (1999) Esca (black measles) and brown wood-streaking: two old and elusive diseases of grapevines. *Plant Dis* **83**: 404–418.
- Murray, A.C., and Woodward, S. (2007) Temporal changes in functional diversity of culturable bacteria populations in Sitka spruce stumps. *For Pathol* **37**: 217–235.
- Mutawila, C., Halleen, F., and Mostert, L. (2016) Optimisation of time of application of *Trichoderma* biocontrol agents for protection of grapevine pruning wounds. *Aust J Grape Wine Res* **22**: 279–287. <https://doi.org/10.1111/ajgw.12218>.
- Nelson, D.M., Glawe, A.J., Labeda, D.P., Cann, I.K.O., and Mackie, R.I. (2009) *Paenibacillus tundrae* sp. nov. and *Paenibacillus xylanexedens* sp. nov., psychrotolerant, xylan-degrading bacteria from Alaskan tundra. *Int J Syst Evol Microbiol* **59**: 1708–1714.
- Noll, M., and Jirjis, R. (2012) Microbial communities in large-scale wood piles and their effects on wood quality and the environment. *Appl Microbiol Biotechnol* **95**: 551–563.
- Oh, H.N., Lee, T.K., Park, J.W., No, J.H., Kim, D., and Sul, W.J. (2017) Metagenomic SMRT sequencing-based exploration of novel lignocellulose-degrading capability in wood detritus from *Torreya nucifera* in Bija forest on Jeju Island. *J Microbiol Biotechnol* **27**: 1670–1680.
- Okonechnikov, K., Conesa, A., and García-Alcalde, F. (2015) Qualimap 2: advanced multi-sample quality control for high-throughput sequencing data. *Bioinformatics* **32**: 292–294. <https://doi.org/10.1093/bioinformatics/btv566>.
- Ouadi, L., Bruez, E., Bastien, S., Yacoub, A., Coppin, C., Guérin-Dubrana, L., et al. (2021) Sap flow disruption in grapevine is the early signal predicting the structural, functional and genetic responses to Esca disease. *Front Plant Sci* **12**: 695846. <https://doi.org/10.3389/fpls.2021.695846>.
- Park, S., Johnson, D.K., Ishizawa, C.I., Parilla, P.A., and Davis, M.F. (2009) Measuring the crystallinity index of cellulose by solid state ¹³C nuclear magnetic resonance. *Cellulose* **16**: 641–647. <https://doi.org/10.1007/s10570-009-9321-1>.
- Parks, D.H., Chuvochina, M., Waite, D.W., Rinke, C., Skarshewski, A., Chaumeil, P.A., and Hugenholtz, P. (2018) A standardized bacterial taxonomy based on genome phylogeny substantially revises the tree of life. *Nat Biotechnol* **36**: 996–1004. <https://doi.org/10.1038/nbt.4229>.
- Parks, D.H., Imelfort, M., Skennerton, C.T., Hugenholtz, P., and Tyson, G.W. (2015) CheckM: assessing the quality of microbial genomes recovered from isolates, single cells, and metagenomes. *Genome Res* **25**: 1043–1055.
- Pasquier, G., Lapaillerie, D., Vilain, S., Dupuy, J.W., Lomelech, A.M., Claverol, S., and Donèche, B. (2013) Impact of foliar symptoms of “Esca proper” on proteins related to defense and oxidative stress of grape skins during ripening. *Proteomics* **13**: 108–118. <https://doi.org/10.1002/pmic.201200194>.
- Péros, J.P., Berger, G., and Jammaux-Despreaux, I. (2008) Symptoms, wood lesions and fungi associated with esca in organic vineyards in Languedoc-Roussillon (France). *J Phytopathol* **156**: 297–303.
- Pinto, C., Pinho, D., Sousa, S., Pinheiro, M., Egas, C., and Gomes, A. (2014) Unravelling the diversity of grapevine microbiome. *PLoS One* **9**: e85622.
- Probst, M., Gómez-Brandón, M., Bardelli, T., Egli, M., Insam, H., and Ascher-Jenull, J. (2018) Bacterial communities of decaying Norway spruce follow distinct slope exposure and time-dependent trajectories. *Environ Microbiol* **20**: 3657–3670.

- Purahong, W., Arnstadt, T., Kahl, T., Bauhus, J., Kellner, H., Hofrichter, M., *et al.* (2016) Are correlations between deadwood fungal community structure, wood physico-chemical properties and lignin-modifying enzymes stable across different geographical regions? *Fungal Ecol* **22**: 98–105. <https://doi.org/10.1016/j.funeco.2016.01.002>.
- Redford, A.J., Bowers, R.M., Knight, R., Linhart, Y., and Fierer, N. (2010) The ecology of the phyllosphere: geographic and phylogenetic variability in the distribution of bacteria on tree leaves. *Environ Microbiol* **12**: 2885–2893.
- Rezgui, A., Ben Ghnaya-Chakroun, A., Vallance, J., Bruez, E., Hajlaoui, M.R., Sadfi-Zouaoui, N., and Rey, P. (2016) Endophytic bacteria with antagonistic traits inhabit the wood tissues of grapevines from Tunisian vineyards. *Biol Control* **99**: 28–37. <https://doi.org/10.1016/j.biocontrol.2016.04.005>.
- Seemann, T. (2014) Prokka: rapid prokaryotic genome annotation. *Bioinformatics* **30**: 2068–2069.
- Serra, S., Borgo, M., and Zanzotto, A. (2000) Investigation into the presence of fungi associated with esca of young vines. *Phytopathol Mediterr* **39**: 21–25.
- Sparapano, L., Bruno, B., Ciccarone, C., and Graniti, A. (2000) Infection of grapevines by some fungi associated with esca. I. *Fomitiporia punctata* as a wood-rot inducer. *Phytopathol Mediterr* **39**: 46–52.
- Sparapano, L., Bruno, G., and Graniti, A. (2001) Three year observation of grapevines cross-inoculated with esca associated fungi. *Phytopathol Mediterr* **40**: S376–S386.
- Tláškal, V., Zrůstová, P., Vrška, T., and Baldrian, P. (2017) Bacteria associated with decomposing dead wood in a natural temperate forest. *FEMS Microbiol Ecol* **93**: fix157.
- Tramoy, R., Sebilo, M., Tu, T., and Schnyder, J. (2017) Carbon and nitrogen dynamics in decaying wood: Paleo environmental implications. *Environ Chem* **14**: 9–18. <https://doi.org/10.1071/EN16049>.
- Úrbez-Torres, J.R., and Gubler, W.D. (2009) Pathogenicity of *Botryosphaeriaceae* species isolated from grapevine cankers in California. *Plant Dis* **93**: 584–592.
- Valášková, V., de Boer, W., Gunnewiek, P., Pospisek, M., and Baldrian, P. (2009) Phylogenetic composition and properties of bacteria coexisting with the fungus *Hypholoma fasciculare* in decaying wood. *ISME J* **3**: 1218–1221.
- Weber, T., Blin, K., Duddela, S., Krug, D., Kim, H.U., Brucoleri, R., *et al.* (2015) antiSMASH 3.0 a comprehensive resource for the genome mining of biosynthetic gene clusters. *Nucleic Acids Res* **43**: W237–W243.
- West, E.R., Cother, E.J., Steel, C.C., and Ash, G.J. (2010) The characterization and diversity of bacterial endophytes of grapevine. *Can J Microbiol* **56**: 209–216.
- Zhu, S., Hegemann, J.D., Fage, C.D., Zimmermann, M., Xie, X., Linne, U., and Marahiel, M.A. (2016) Insights into the unique phosphorylation of the lasso peptide paeninodin. *J Biol Chem* **291**: 13662–13678.
- Zimmermann, W. (1990) Degradation of lignin by bacteria. *J Biotechnol* **13**: 119–130.

Supporting Information

Additional Supporting Information may be found in the online version of this article at the publisher's web-site:

Table S1. RAST annotation of S150.

Table S2. eggnoG annotation of S150.

Table S3. Glycoside hydrolases genes present in the genome of strain S150. GH: Glycoside hydrolases.

Table S4. protein encoding genes predicted to be involved in plant-microbe interaction by strain S150 determined by RAST.

Table S5. protein encoding genes predicted to be involved in oxidative stress and detoxification of strain S150 determined by RAST.

Table S6. protein encoding genes predicted to be involved in resistance to antibiotics and toxic compounds of strain S150 determined by RAST.

Fig. S1. Degradation of wood component by A: *F. mediterranea* a) cellulose b) xylan c) lignin; B) bacteria; a) cellulose b) xylan c) lignin (absence of halo)

Fig. S2. Effect of the presence of wooden rods on the growth rate of *F. mediterranea*. Three days culture of *F. mediterranea* on MA with (A) or without wooden rod (B).